Chapter 5

A novel force myography sensor to measure muscle contraction for controlling hand prosthesis

5.1 Introduction

Non-invasive assessment of muscle contraction has extensive applications in the diagnosis of neuromuscular disorders, muscle fatigue analysis, controlling prosthetics, etc. (Spires, Kelly, and Davis 2014; Lobo-Prat et al. 2014; Veer and Sharma 2018; Veer 2015; Sharma and Veer 2016). Contraction can be measured by monitoring the electrical or mechanical activity of the muscle(Schoening 1986). Surface electromyography (sEMG) is the most frequently used technique for quantifying the electrical activity of muscles underlying the skin. Nowadays, EMG measurement (from voluntary muscle contraction) is widely utilized for active prosthesis control and other human-machine interfaces (HMI) due to its intuitiveness (Tavakoli, Benussi, and Lourenco 2017; Pancholi and Joshi 2018; Veer, Agarwal, and Kumar 2016).

Surface electromyography involves the use of myoelectrodes, which provide the crude assessment of EMG signal under the skin and appropriate pre-processing circuitry to obtain amplified as well as a filtered version of the signal directly from the electrodes(Veer 2014). The correct measurement of the EMG signal involves the proper placement of electrodes with good electrical interaction with the skin (Schoening 1986; Day, 2002; Chowdhury et al. 2013). Conductive gel-based electrodes can achieve a good and steady electrical contact with the skin, but for long-term application, dry electrodes are preferred(Jamal and Kim 2018). However, dry electrodes offer high electrode-skin impedance and are also susceptible to motion artifacts (Searle and Kirkup 2000). The EMG signal quality is dependent on the anatomy and physiology of the muscle-skin interface and the signal conditioning circuitry of the detection unit. Moreover, the acquisition of EMG signals is very sensitive to the various noise sources (Chowdhury et al. 2013; Amrutha and Arul 2017). These noises, up to a great extent, can be minimized using appropriate pre-processing circuitry, post-processing techniques, and

effective training schemes but cannot be eliminated (Hargrove, Englehart, and Hudgins 2008; Naik et al. 2016).

The activity of muscle can also be monitored by detecting the changes in mechanical features during contraction. Muscle contraction leads to shortening of the muscle, change in cross-section areas, increase in toughness, and increases the mechanical vibrations associated with the muscle. Mechanomyography (MMG), optomyography (OMG), and force myography (FMG) are some of the measurement techniques for identifying these mechanical variations occurring during muscular contraction. MMG is measured as the mechanical vibrations produced by the muscle during its activation (Ibitoye et al. 2014). It can be considered as the mechanical equivalent of the EMG signal. Accelerometers, piezoelectric sensors, microphones, and LASER distance sensors are various sensors for assessing the MMG signal. There are some case studies in which MMG signal has been characterized for analyzing muscle function, prosthesis control, identifying neuromuscular diseases, and evaluation of muscle during sports and medicine (M. A. Islam et al. 2013). MMG has several advantages over EMG, such as simple acquisition setup, high signal-to-noise ratio (SNR), and resistant to external electromagnetic interference. However, it is more sensitive to movement artifacts than the EMG signal, which can significantly influence results (Woodward et al. 2019; A. Islam et al. 2012). OMG is another new approach that utilizes photoelectric sensors for detecting mechanical variations of muscle during contraction. It offers higher SNR and enhanced robustness against the undesired features and limitations of MMG and EMG (Hamed Hamid Muhammed and Raghavendra, 2014). OMG can provide a cheap and contactless assessment of muscular contraction that can be efficiently utilized to generate the control signal for upper-limb prosthesis and other rehabilitation applications (H. H. Muhammed and Jammalamadaka

2016). But as compared to the EMG, the OMG signal is more affected by motion artifacts and also exhibits slight delay, which may affect the performance for real-time control applications (Chianura and Giardini 2010; “An IR Muscle Contraction Sensor” 2014.).

FMG is a recently developed technique that utilizes force-sensitive resistors (FSRs) to register the volumetric changes of muscle during its activity. Unlike EMG, FMG is inexpensive, simple to use, insensitive to external electrical interference, does not requires the use of electrodes and complex conditioning circuits (Jiang et al. 2017; Yaniger 1991). Moreover, FMG produces a more repeatable pattern and shows higher overall stability over time than EMG (Jiang et al. 2017; Connan et al. 2016). FMG can provide an assessment of muscular contraction that can be efficiently utilized to generate the control signal for upper-limb prosthesis and other rehabilitation applications. In recent applications, FMG based control system has gained much attention for the utilization of prosthetic devices (Cho et al. 2016; Ha, Withanachchi, and Yihun 2019; Radmand, Scheme, and Englehart 2016; Li et al. 2012; Zhen G Xiao and Menon 2014). The overall realization of the FMG system is less expensive as it requires fewer FSRs than the EMG system, which involves large numbers of electrodes for detecting distinct gestures of muscle activity(Ha, Withanachchi, and Yihun 2019).

However, previous studies reported that the direct use of FSR on the skin could only furnish qualitative information about muscle activation. The simple FSR element cannot provide quantitative details like how the FSR output is related to the intensity of contractions and the comparative analysis with other sensors. They only supply the basic information about the activation and relaxation of the muscle (Lukowicz et al. 2006; Junker et al. 2008). Also, using a basic voltage divider as a conditioning circuit for FSR produces nonlinearities, large drift errors, and variation in sensitivity over its operating range. These errors and nonlinearities

could be minimized using suitable electronic conditioning circuitry and signal processing systems, (Kalantari et al. 2012; Matute et al. 2018).

Despite having several advantages, FMG is still unpopular for the application of prosthesis control. The main reasons are instability of the sensor on the skin, the inconsistent transmission of muscular contractile force onto the sensor, wearability, reliability, robustness, cost, accessibility, etc.(Esposito et al. 2018).

This chapter presents a novel FMG sensor for faithfully detecting the muscle contraction to be applied for hand prosthesis control. The sensor is designed using a pair of FSR elements mounted inside a 3D printed chassis, which receives muscular contractile force through hemispherical elastomer couplers (prepared from PDMS). The sensor also includes a specific conditioning circuit (with an appropriate power supply) for producing a voltage output proportional to the intensity of contraction. The sensor is simple, compact, sensitive, and easily attachable on the residual upper limb of amputees to reliably capture the mechanical activity of muscle. The sensor produces an output signal comparable to the linear envelope of the EMG signal. The designed sensor was successfully tested on five different human subjects to control a 3D printed prosthetic hand for performing grasping operations utilizing the proportional scheme. The sensor was able to provide a smoother and faster operation of the prosthetic device than a conventional EMG sensor.

5.2 Materials and Methods

5.2.1 Design of FMG Sensor

Contraction leads to the change in volume and stiffness of the muscle, which imparts outward forces. These forces can be sensed through FSR by placing it on the skin in conjunction with

a sensitive portion of the muscle. However, the direct placement of FSR on the skin (i.e., without any mechanical coupler) may provide unreliable and ambiguous results.

FSR mainly consists of a conductive polymer, which shows the piezoresistive effect (i.e., a decrease in resistance with an increase in applied force to its active area). Figure 5.1 shows the different layers of FSR-402, which are a semiconductive layer, spacer adhesive, and the conductive layer ("FSR Integration Guide"). Direct interaction of the FSR element on the skin will exert uneven force on its sensing area and prevent the semiconductive layer from making proper electrical contact with the conductive polymer. In this situation, the output produced by the FSR may not provide the exact amount of force that was applied. There should be an assembly that will provide uniform distribution of muscular contractile force over the sensing portion (active area) of the FSR for getting reliable output from it. Such an arrangement can be achieved using an appropriate size elastomer between the applied force and the FSR active area. Because as long as the force distribution is uniform, the repeatability of the device will be preserved.

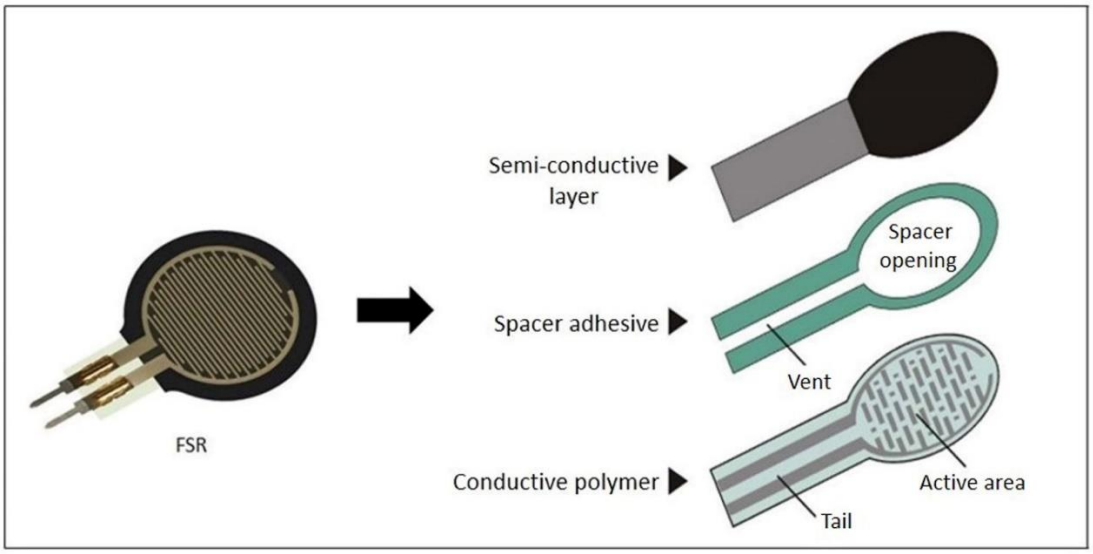

Figure 5.1 Construction of FSR showing its different layers.

A specific mechanical assembly consisting of an elastomer coupler and a 3D printed base was designed for the even transmission of muscular contractile force on the FSR sensing portion. The coupler was made using polydimethylsiloxane (PDMS) material and was moulded into a hemispherical shape of 1.27 cm diameter ("FSR Integration Guide"). PDMS has wide applications in fabrications and characterization of electronic circuits as well as materials and offers advantages such as chemical stability, biocompatibility, transparency, flexibility, thermal conductivity, etc. (Chen et al. 2018; Kim, Lee, and Choi 2013). The flat surface of the coupler was positioned onto the FSR active area, while its convex portion was intended for sensing force directly from the skin. The FSR element, along with the coupler, was mounted inside a 3D printed chassis, as shown in Figure 5.2. The rigid base made of polylactic acid (PLA) provides back support to the FSR plate by preventing its inappropriate bending and promotes uniform distribution of force over the sensing area. When the sensor assembly is attached to the subject, the convex part creates slight subsidence to the skin, making the device a bit more sensitive to detect even the shorter contraction of the muscle. When the muscle is contracted, it imparts a uniform force on the FSR sensing area through the hemispherical coupler. The chassis, FSR plate, elastomer coupler, and conditioning circuitry constitute an FMG sensor that can be attached to forearm muscles using Velcro tape or belt. The FMG sensor comprises a pair of FSRs which can simultaneously detect the contractions occurring at two different target muscle in the range of 3 cm distance.

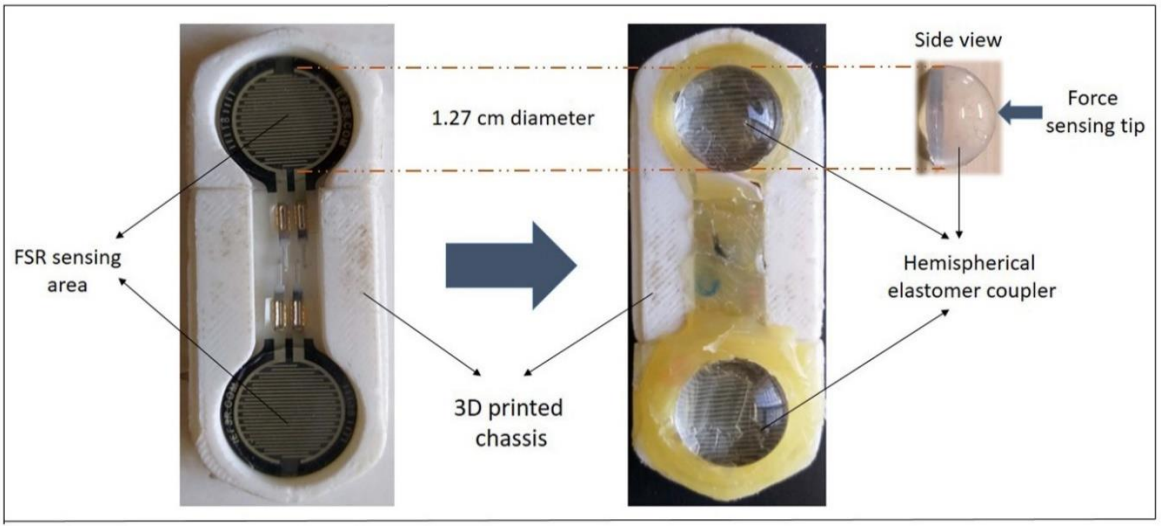

Figure 5.2 Mechanical arrangement for uniform distribution of force on the FSR.

5.2.2 Signal conditioning

The buffered voltage divider circuit is shown in Figure 5.3(a) is the most common circuit for translating the change in resistance of FSR to the voltage output (Amft et al. 2006). A fixed supply voltage is applied across the series combination of FSR and reference resistor (R_1) while the output voltage is measured across R_1. The circuit gives a non-linear relationship between resistance and voltage, which is clear from equation (5.1). The value of R_1 is appropriately selected to achieve the desired force sensitivity of the FSR. A buffer is employed after the voltage divider to fulfill the impedance requirements of the measuring circuit. However, in a practical situation, the voltage divider arrangement in the circuit is unable to maintain a constant voltage drop across the FSR, which may affect accuracy, sensitivity, drift, and repeatability in measurement (Matute et al. 2018). Thus, the use of voltage dividers in the signal conditioning circuitry is less preferred.

$$V_{out} = \frac{R_1 V_{cc}}{(R_1 + R_{FSR})} \tag{5.1}$$

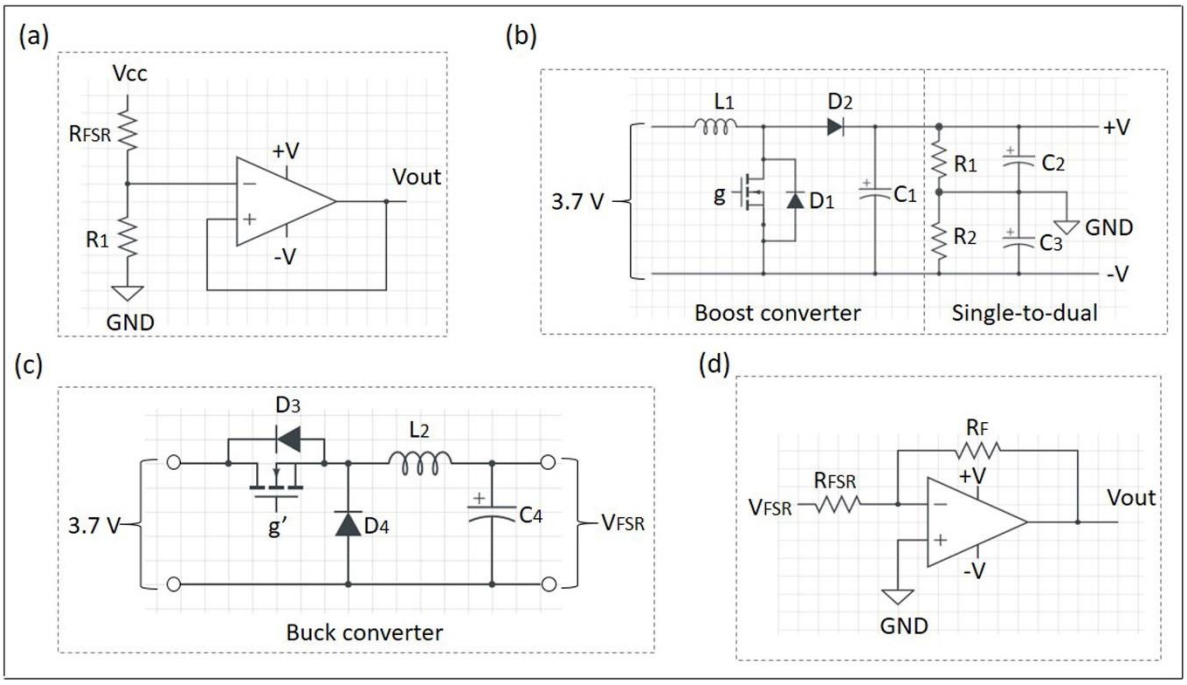

Figure 5.3 (a) Buffered voltage divider, (b) bipolar supply circuitry, (c) buck converter, (d) transimpedance amplifier.

A transimpedance amplifier circuit shown in Figure 5.3 (d) permits a fixed voltage across FSR, making sensitivity constant for a wide range of input forces. If the value of V_{FSR} (i.e., the supply voltage to FSR) in equation (5.2) is kept smaller than 200 mV, drift tends to increase, and there exists a non-linear relationship between FSR output voltage and current (Matute et al. 2018; Paredes-Madrid et al. 2018). While if the supply voltage is increased, the drift reduces, and some linear relationship starts to build up. Moreover, increasing the supply voltage above 2 V will lead to the degradation of FSR sensitivity non-linearly (Lebosse et al. 2011). The sensor should have constant sensitivity over time, such that repetitive muscular contractions can be easily observed. Therefore, the supply voltage was fixed to a trade-off value of 1.85 V to preserve the FSR's sensitivity and minimize the drift. FSR drift and sensitivity degradation cannot be eliminated but can be efficiently reduced using suitable conditioning circuits, as implemented in this work. The value of feedback resistance R_F was chosen 10 kΩ to attain the desired sensitivity ("FSR Integration Guide").

$$V_{out} = \frac{-V_{FSR}}{(R_{FSR})} \times R_F \quad (5.2)$$

In Figure 5.3(b), 3.7 V from the battery was first increased to 10 V using a boost converter circuit and then transformed to a bipolar supply of ±5 V employing a single-to-dual circuit for powering the operational amplifier IC present within the signal conditioning. A buck converter circuit is shown in Figure 5.3(c) was incorporated to supply a constant input (1.85 V) to FSR. All the signal conditioning circuitry and the power supply unit were embedded in the sensor chassis for making it a standalone device.

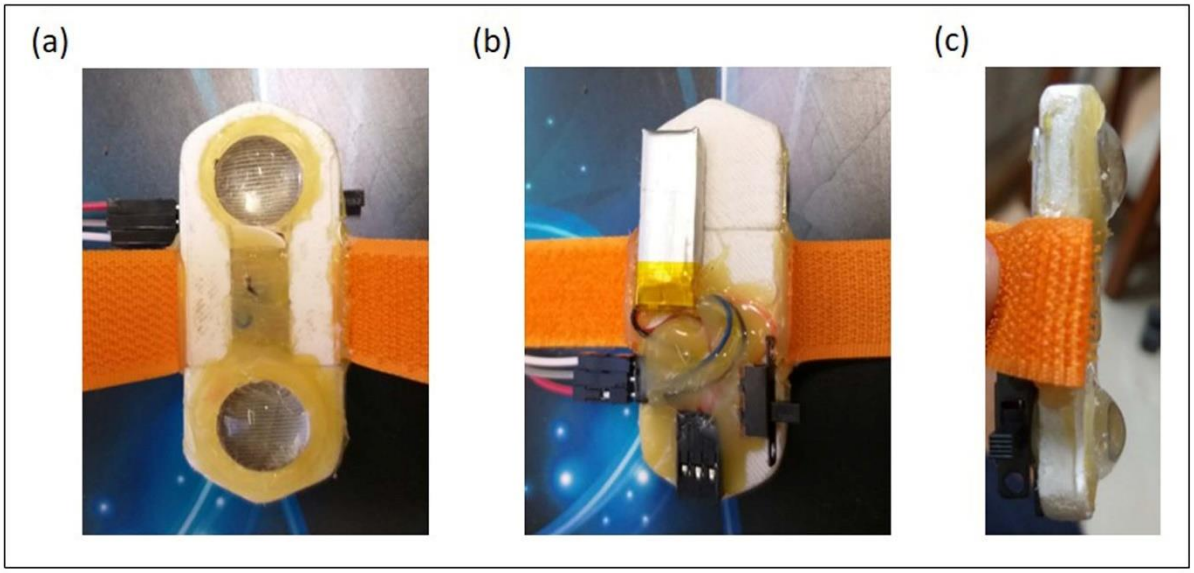

Figure 5.4 Designed FMG sensor (a) front view, (b) rear view, (c) side view.

The final output produced by the transimpedance amplifier is a 0-5 V linear envelope proportional to the strength (force) of contraction. The designed FMG sensor can provide two-channel output since it comprises two FSR elements and their signal conditioning units and power supply. A single pole double throw (SPDT) switch was incorporated for powering on the sensor. Figure 5.4(a) and 5.4(c) show the front and side views of the designed FMG sensor showing the hemispherical tip for sensing the muscular contractions on the skin, whereas Figure 5.4(b) shows the rearview consisting of the switch, connectors, and battery.

5.2.3 Static and dynamic characteristics of the FMG sensor

Static calibration for the developed sensor was performed to quantify the relation between applied force and output voltage. For this, different weights were applied perpendicularly on the hemispherical tip (active area) of the sensor one by one, and the output voltages were recorded. The output voltages were recorded for 120 s after the application of static loads to measure the actual drift attained by the sensor. The drift was calculated as a percentage of variation in the sensor's output voltage from the predicted value, as per the equation (5.3).

$$Drift(t) = \frac{V_o(t) - V_o(0)}{V_o(0)} \times 100 \quad (5.3)$$

Where $V_o(t)$ is the voltage output of the sensor at a time 't' and $V_o(0)$ the voltage output of the sensor immediately after the application of load (i.e., the predicted value).

Hysteresis error for the developed sensor was analyzed through variation of output voltage with the increasing and decreasing intensity of applied weight (i.e., loading and unloading).

The repeatability error of the sensor was evaluated for five repeated applications of the same load on the sensor. It was determined as a percentage of relative standard deviation (RSD) calculated for the application of eleven different weights. RSD can be calculated using the formula in equation (5.4).

$$RSD = \frac{\sqrt{((X - \bar{X}))/n}}{\bar{X}} \times 100 \quad (5.4)$$

Where $\bar{X}$ is the mean value of data samples, X is any value in the data samples, and n is the number of samples.

The dynamic characteristic of the sensor was analyzed in terms of its frequency response, which was determined experimentally to test its ability to record rapidly varying FMG signals. A specific arrangement shown in Figure 5.5 was made to measure the sensor's magnitude and

phase response at different mechanical frequencies. A mini electrodynamic shaker (model 2007E from Modal shop) was fixed on the table such that its vibration tip makes direct contact with the hemispherical sensing tip of the FMG sensor, which was held vertical using a vise. An accelerometer (ADXL345) was fixed to the upper part of the vibration tip of the shaker for measuring its acceleration.

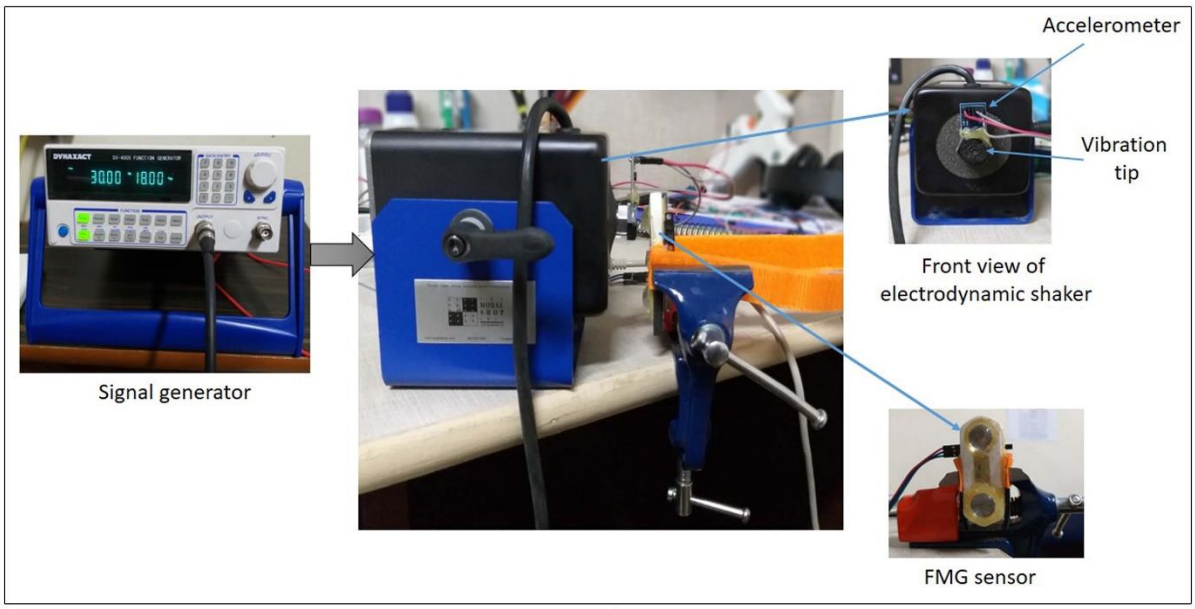

Figure 5.5 Experimental arrangement for the measurement of the frequency response of the designed FMG sensor.

The mini shaker was stimulated with a sinusoidal voltage (18 V) of increasing frequency (i.e., 1 Hz to 3 MHz) using a function generator (DX-4005). The FMG sensor data and the accelerometer data were simultaneously acquired using a data acquisition (DAQ) device (Advantech, USB-4716) during the vibrations at different frequencies. All the data were acquired at a sampling frequency of 2 kHz. Since the weight of the shaker and accelerometer assembly is fixed, the actual force applied to the sensor was calibrated in terms of voltage using the acceleration produced by the accelerometer. The gain magnitude of the frequency response was determined as the ratio of FMG sensor output (in voltage) to the actual force computed

from the accelerometer data. At the same time, the phase magnitude of the frequency response was determined by calculating the time-lag between the positive-slope zero-crossings of the actual sinusoidal force applied and the voltage output of the FMG sensor (Esposito et al. 2018).

5.2.4 Similarity with the EMG signal

In order to accomplish a quantifiable comparison between the developed FMG sensor and traditional EMG sensor, simultaneous measurements of FMG and EMG signals were performed for eight subjects (five healthy and three transradial amputees) from their forearm muscles. The FMG sensor and the EMG sensor were placed close to each other on the flexor carpi ulnaris muscle, as shown in Figure 5.6, as this muscle on the forearm is responsible for the movement of the wrist and fingers (Lobo-Prat et al. 2014; Supuk, Skelin, and Cic 2014). The curved sensing tip of the FMG sensor was positioned on the belly of the muscle such that any contraction can be easily detected.

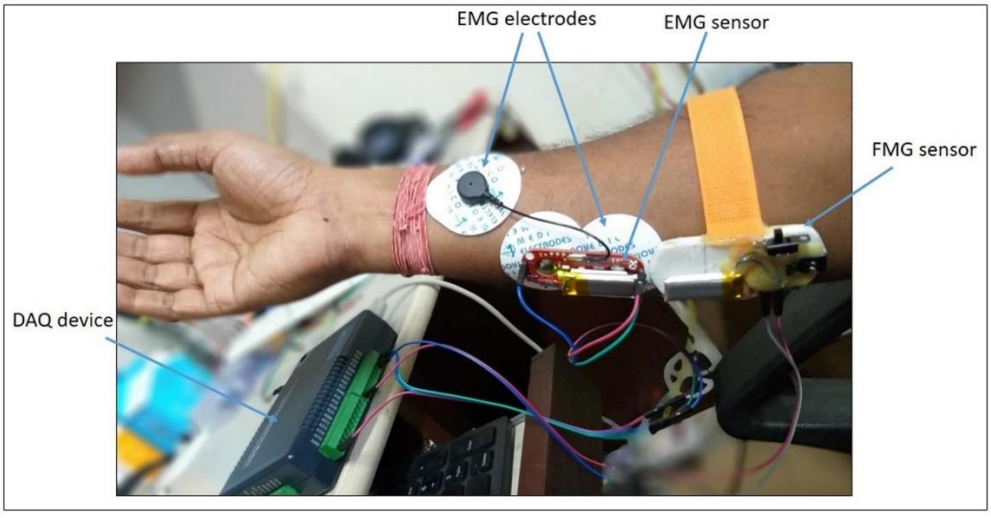

Figure 5.6 Placement of FMG sensor and EMG sensor on the forearm muscle of a subject.

The employed EMG sensor (i.e., myoware muscle sensor from advancer technologies) can provide the raw as well as the linear envelope of the EMG signal. The signals using both the

sensors were simultaneously acquired using the DAQ device at a sampling frequency of 2 kHz with 16-bit precision. The subjects were asked to perform voluntary muscle contractions of different duration and intensities.

5.2.5 Controlling hand prosthesis

The ability of the designed FMG sensor was further tested for controlling hand prosthesis implementing a proportional control scheme. A five-fingered, 3D printed hand was prepared, which was extrinsically actuated using two high torque servomotors (MG-995) (Kargov et al. 2004). The hand includes the microcontroller circuit, which controls the actuators using input signals from different sources like EMG devices, force sensors, switches, etc. A 2000 mAh lithium-polymer battery was integrated into the hand assembly for supplying power to servomotors and the microcontroller. Silicon caps were installed on the fingers to enhance the grasping capability of the 3D printed hand.

The proportional control scheme was realized, which provides actuation of the prosthetic hand fingers according to the intensity of the input signal from muscular contraction (Farina et al. 2014). Such a scheme offers intuitive control and faster-grasping capability to the hand (Fougner et al. 2012).

First, the prosthetic hand operation was performed using the EMG control signal, after which it was done utilizing FMG sensor control. Amputees sequentially wore both the sensors on their forearm muscle (i.e., flexor carpi radialis muscle) and performed some basic operations like opening/closing and grasping simple and delicate objects with the developed prosthetic hand. Response time (closing/opening time) of the prosthetic hand with both the sensors were obtained from the recorded video of hand operation to see the ability of sensors in producing a faster control signal. Figure 5.7 shows the attachment of the designed FMG sensor on the

residual forearm stump of an amputee for controlling the operation of a 3D printed hand prototype.

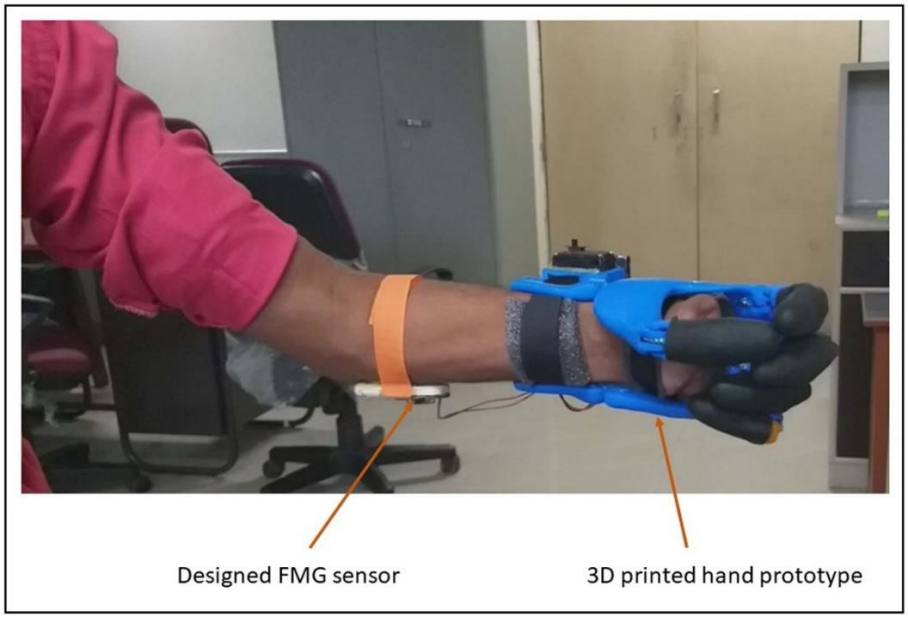

Figure 5.7 Controlling 3D printed hand prosthesis using the FMG signal of an amputee.

5.3 Results and discussion

5.3.1 Static and dynamic results

The static calibration curve for the designed FMG sensor is shown in Figure 5.8. From the obtained curve, it can be concluded that the sensor's sensitivity remains almost constant over a lower range of input weight and starts to vary as weight increases above a specific value. The sensor is more sensitive to lighter loads as compared to heavier loads. The designed sensor can be a good option for detecting the shorter to larger muscular contractions of forearm muscles based on this feature.

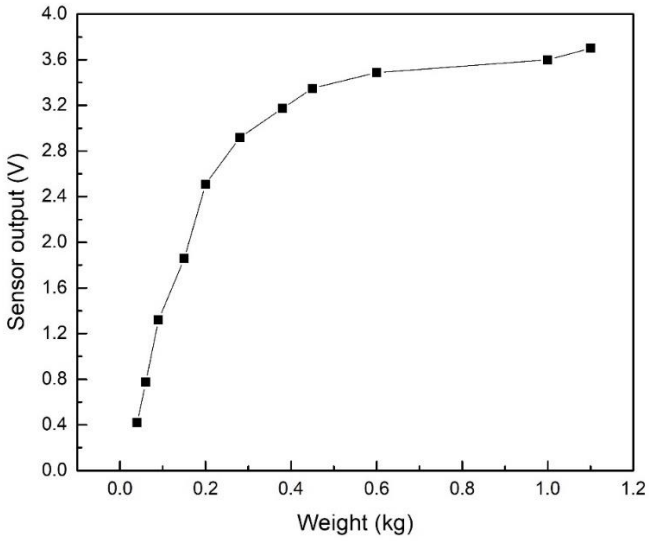

Figure 5.8 Static calibration curve for the FMG sensor.

For the application of different static loads, the developed sensor output was recorded for 120 s, whose variation is shown in Figure 5.9. The drift error was determined with all the weights applied on the sensor for 120 s. Variation of drift error in percentage for all the applied weights is shown in Figure 5.10. The drift error has no relation with the loads; however, its value is always confined below 7 %. This feature of the sensor is acceptable as per the datasheet of FSR.

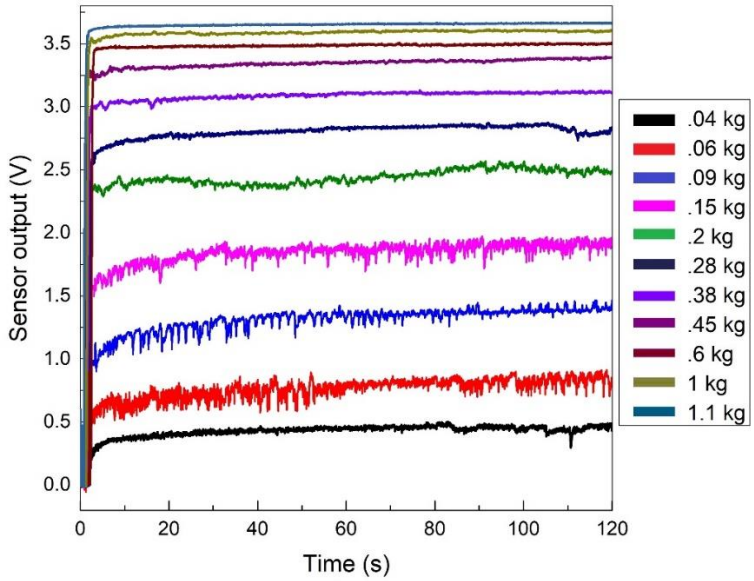

Figure 5.9 Recorded output of the sensor for 120 s after application of different static loads.

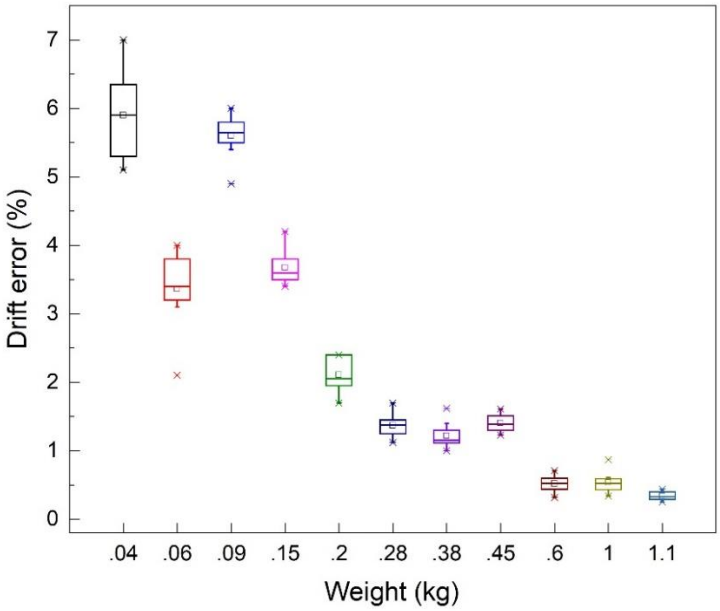

Figure 5.10 FMG sensor drift error at different applied weights.

The hysteresis curve shown in Figure 5.11 was obtained through the variation of output voltage with the increasing and decreasing strength of applied weight. The average hysteresis error calculated for the sensor was 6 %.

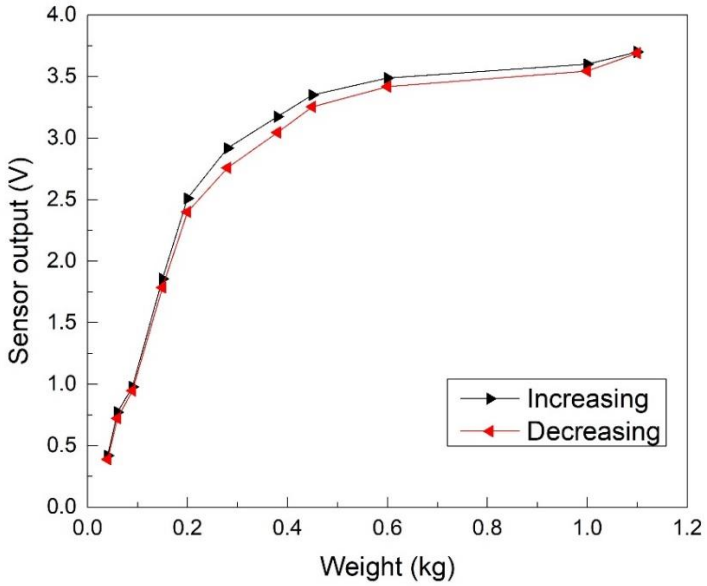

Figure 5.11 Hysteresis curve obtained for the sensor.

Repeatability error for the sensor considering all the applied loads analyzed in terms of RSD percentage is described in Figure 5.12. The determined average repeatability error for the sensor was 3 %. However, the variation of RSD percentage was found larger for lighter loads. The obtained frequency response curve for the designed sensor is depicted in Figure 5.13. There are a flat amplitude response and linear phase, up to 400 Hz. A resonance peak was detected at about 800 Hz. Therefore bandwidth of the sensor is sufficient to characterize the rapidly varying FMG signal correctly, as the FMG spectrum for humans varies from 1-500 Hz (Zhen Gang Xiao and Menon 2019).

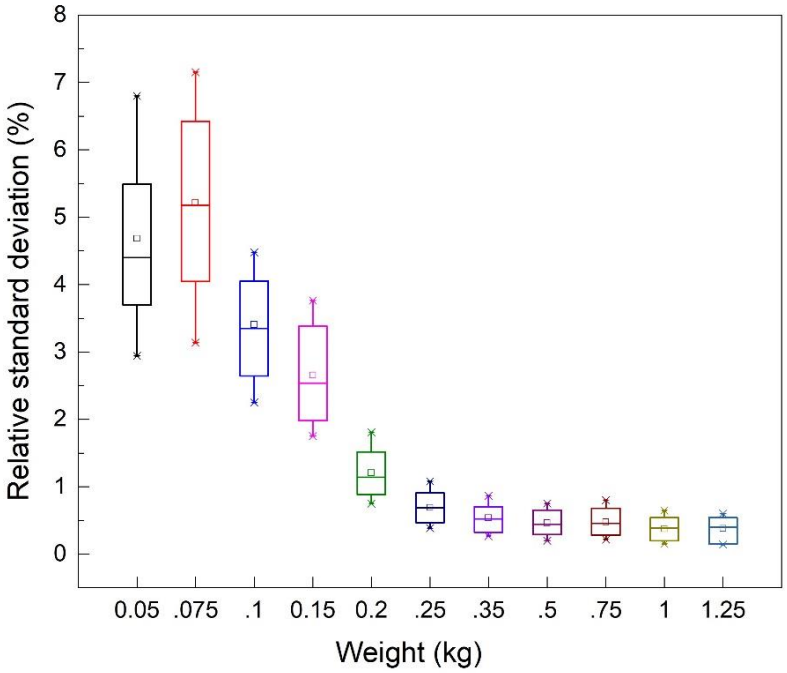

Figure 5.12 Repeatability error of the sensor at different loads.

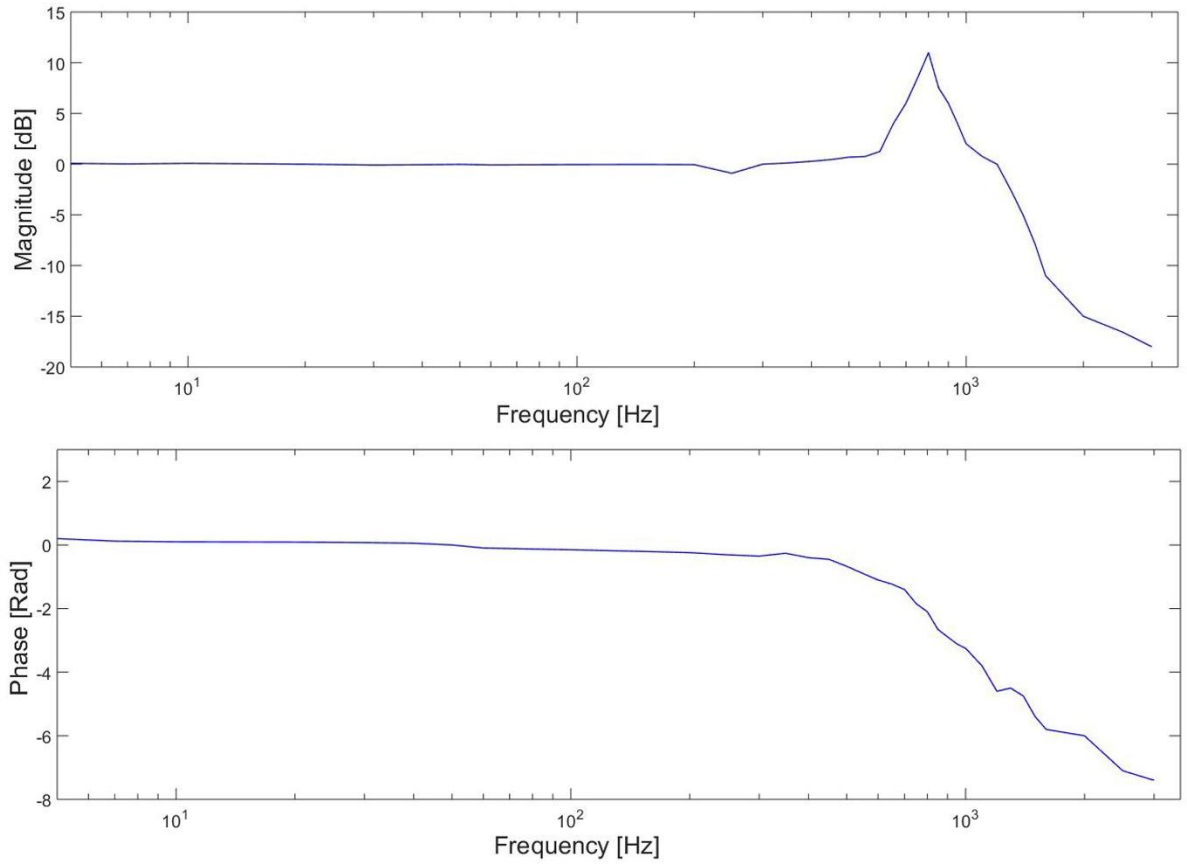

Figure 5.13 Dynamic response of the sensor: magnitude frequency response (upper panel) and phase frequency response (lower panel).

5.3.2 EMG-FMG comparison

The following results were obtained when subjects performed contraction of their forearm muscles with different intensities by flexing their fingers at a different strength. Figure 5.14 shows simultaneously recorded raw EMG signal, its linear envelope, and FMG signal from the sensors for three different muscular contractions of decreasing intensity of a healthy subject. The first contraction represents the maximum voluntary contraction (MVC), while the other two contractions correspond to 50 % and 25 % of MVC. The EMG linear envelope was considered a percentage of MVC, whereas FMG signals were measured in volts.

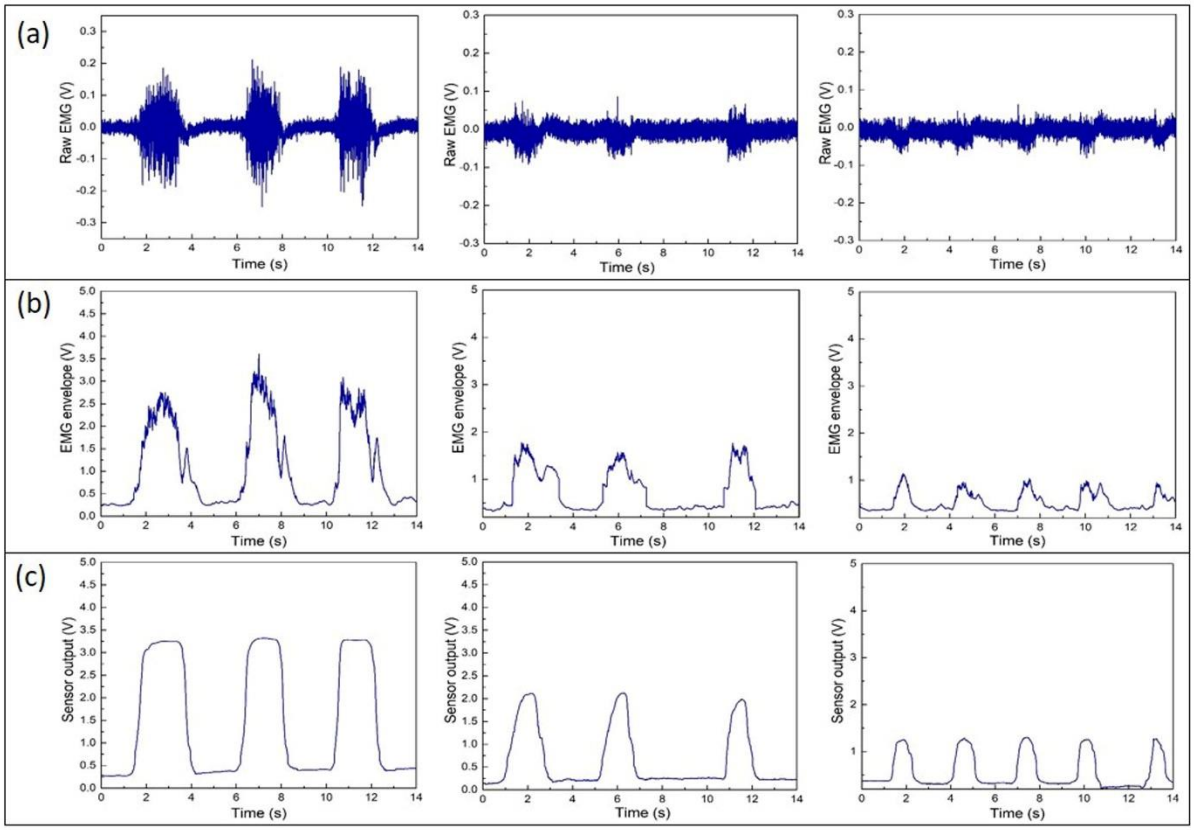

Figure 5.14 Simultaneous recordings of (a) raw EMG signal, (b) linear envelope of EMG, (c) FMG sensor output for three different contractions of forearm muscle of decreasing intensity.

A good similarity was observed between the EMG linear envelope and the signal produced by the FMG sensor. A two-tailed paired t-test was performed between these two signals for quantitatively analyzing their similarity. The result showed a high Pearson's correlation coefficient ($r > 0.87$) with a p-value < 0.0001 exhibiting the pairing was significantly effective. The similarity test was done using data of eight subjects for their total twenty-four contractions.

However, at the end of the contraction EMG signal showed a delay with respect to the FMG signal. This delay is mainly due to the envelope detection stage involved in the EMG conditioning circuitry(D'Alessio and Conforto 2001).

5.3.3 Hand prosthesis control

The linear envelope of the EMG signal was first utilized to control the prosthetic hand implementing a proportional control scheme. Further, the FMG control signal was used instead of an EMG signal for executing various hand operations (Figure 5.15). A total of three amputees and two healthy subjects participated in this trial and were asked to perform grasping of objects of daily livings with the 3D printed hand. The subjects were able to accomplish the assigned hand activities and reported no considerable differences between the EMG control and FMG control of the prosthetic hand. Subjects also revealed that the designed FMG sensor was easier and more comfortable to wear than the EMG sensor, which requires gelled electrodes.

Figure 5.15 Different grasping operations performed by an amputee wearing a hand prosthesis.

Moreover, the closing/opening time of the prosthetic hand with the EMG sensor was computed 450/550 ms, while with the FMG sensor, it was 350/300 ms. This result shows that the FMG control provides a faster operating speed of the prosthetic device than the EMG control.

Therefore based on these preliminary tests and results, it can be concluded that the designed FMG sensor can become an excellent alternative to the EMG device for controlling a prosthetic hand.

5.4 Conclusion

In this chapter, a new FMG sensor has been presented that can detect the muscular contraction applied for controlling hand prostheses. The typical mechanical design and signal conditioning circuit of the sensor enables a measurable and reliable detection of muscular contraction compared to earlier research involving simple FSR sensors. The integration of a mechanical coupler, FSR element, conditioning circuitry, and power supply on a single chassis makes the sensor compact, wearable for immediate and long-term use. The designed dual-channel sensor is a low-cost device that provides a non-invasive assessment of muscle activation (under the skin) and produces an output proportional to the intensity of contraction. Also, the sensor does not require the use of electrodes or any electrical interaction with the subject's skin and does not need any pre-processing filters to detect muscular contraction levels as required by the other techniques like EMG or MMG. The designed sensor based on the piezoresistive effect provides a simple and sensitive mode to detect muscular contractions of different intensities. The signal produced by the sensor is comparable to EMG linear envelope and also faster in response.

However, the designed sensor suffers from some static errors like drift and sensitivity errors, which can be minimized by further improvement in the signal conditioning circuitry (Paredes-Madrid et al. 2018; Matute et al. 2018).

The sensor was successfully tested on human subjects for controlling the operation of an intrinsically actuated 3D printed hand prosthesis utilizing the proportional control strategy. The sensor provides faster operation of the prosthetic hand as compared to the conventional EMG sensor.

Such a sensor can effectively monitor the muscular contraction as detected by the EMG device without any effect of noise sources such as electromagnetic interference, motion artifacts, etc., and can be used as an excellent alternative to an EMG sensor for controlling prosthesis or other assistive devices.

The current study deals with a two-channel FMG sensor, which can be possibly expanded to an array of sensors for measuring contractions at multiple locations of muscles and tackling the crosstalk associated with the surrounding muscles. Moreover, the FMG sensor, along with the EMG and MMG sensor, can be effectively applied for diagnosing neuromuscular diseases, studying muscle fatigue, and controlling a multifunctional prosthetic hand.

5.5 References

Amrutha N, Arul VH. A Review on Noises in EMG Signal and its Removal. Int. J. Sci. Res. Publ. 2017 May; 7(5):23-7.

Amft, O., H. Junker, P. Lukowicz, G. Troster, and C. Schuster. 2006. "Sensing Muscle Activities with Body-Worn Sensors." In International Workshop on Wearable and Implantable Body Sensor Networks (BSN'06), 4 pp. – 141. https://doi.org/10.1109/BSN.2006.48.

"An IR Muscle Contraction Sensor." Accessed June 15, 2019. https://people.ece.cornell.edu/land/courses/eceprojectsland/STUDENTPROJ/2013to2014/ras578/Writeup/An%20IR%20Muscle%20Contraction%20Sensor.html.

Chen, Jing, Jiahong Zheng, Qinwu Gao, Jinjie Zhang, Jinyong Zhang, Olatunji Omisore, Lei Wang, and Hui Li. 2018. "Polydimethylsiloxane (PDMS)-Based Flexible Resistive Strain Sensors for Wearable Applications." Applied Sciences 8 (3): 345. https://doi.org/10.3390/app8030345.

Chianura, Alessio, and Mario E. Giardini. 2010. "An Electrooptical Muscle Contraction Sensor." Medical & Biological Engineering & Computing 48 (7): 731–34. https://doi.org/10.1007/s11517-010-0626-x.

Cho, Erina, Richard Chen, Lukas-Karim Merhi, Zhen Xiao, Brittany Pousett, and Carlo Menon. 2016. "Force Myography to Control Robotic Upper Extremity Prostheses: A Feasibility Study." Frontiers in Bioengineering and Biotechnology 4 (March). https://doi.org/10.3389/fbioe.2016.00018.

Chowdhury, Rubana H., Mamun B. I. Reaz, Mohd Alauddin Bin Mohd Ali, Ashrif A. A. Bakar, K. Chellappan, and T. G. Chang. 2013. "Surface Electromyography Signal Processing and Classification Techniques." Sensors (Basel, Switzerland) 13 (9): 12431–66. https://doi.org/10.3390/s130912431.

Connan, Mathilde, Eduardo Ruiz Ramírez, Bernhard Vodermayer, and Claudio Castellini. 2016. "Assessment of a Wearable Force- and Electromyography Device and Comparison of the Related Signals for Myocontrol." Frontiers in Neurorobotics 10 (November). https://doi.org/10.3389/fnbot.2016.00017.

D'Alessio, T., and S. Conforto. 2001. "Extraction of the Envelope from Surface EMG Signals." IEEE Engineering in Medicine and Biology Magazine 20 (6): 55–61. https://doi.org/10.1109/51.982276.

Day, Scott. 2002 "Important factors in surface EMG measurement," Calgary, AB: Bortec Biomedical Ltd Publishers.

Esposito, Daniele, Emilio Andreozzi, Antonio Fratini, Gaetano D Gargiulo, Sergio Savino, Vincenzo Niola, and Paolo Bifulco. 2018. "A Piezoresistive Sensor to Measure Muscle Contraction and Mechanomyography." Sensors (Basel, Switzerland) 18 (8). https://doi.org/10.3390/s18082553.

Farina, Dario, Ning Jiang, Hubertus Rehbaum, Ales Holobar, Bernhard Graimann, Hans Dietl, and Oskar C. Aszmann. 2014. "The Extraction of Neural Information from the Surface EMG for the Control of Upper-Limb Prostheses: Emerging Avenues and Challenges." IEEE Transactions on Neural Systems and Rehabilitation Engineering 22 (4): 797–809. https://doi.org/10.1109/TNSRE.2014.2305111.

Fougner, Anders, Oyvind Stavdahl, Peter J. Kyberd, Yves G. Losier, and Philip A. Parker. 2012. "Control of Upper Limb Prostheses: Terminology and Proportional Myoelectric

Control-a Review." IEEE Transactions on Neural Systems and Rehabilitation Engineering: A Publication of the IEEE Engineering in Medicine and Biology Society 20 (5): 663–77. https://doi.org/10.1109/TNSRE.2012.2196711.

Ha, Nguon, Gaminda Pankaja Withanachchi, and Yimesker Yihun. 2019. "Performance of Forearm FMG for Estimating Hand Gestures and Prosthetic Hand Control." Journal of Bionic Engineering 16 (1): 88–98. https://doi.org/10.1007/s42235-019-0009-4.

Hargrove, Levi, Kevin Englehart, and Bernard Hudgins. 2008. "A Training Strategy to Reduce Classification Degradation Due to Electrode Displacements in Pattern Recognition Based Myoelectric Control." Biomedical Signal Processing and Control, Surface Electromyography, 3 (2): 175–80. https://doi.org/10.1016/j.bspc.2007.11.005.

Ibitoye, Morufu Olusola, Nur Azah Hamzaid, Jorge M. Zuniga, and Ahmad Khairi Abdul Wahab. 2014. "Mechanomyography and Muscle Function Assessment: A Review of Current State and Prospects." Clinical Biomechanics 29 (6): 691–704. https://doi.org/10.1016/j.clinbiomech.2014.04.003.

Interlink Electronics, 2002. FSR Force Sensing Resistor–Integration Guide and Evaluation Parts Catalog.

Islam, Anamul, Kenneth Sundaraj, Badlishah Ahmad, Nizam Uddin Ahamed, and Asraf Ali. 2012. "Mechanomyography Sensors for Muscle Assessment: A Brief Review." Journal of Physical Therapy Science 24 (12): 1359–65. https://doi.org/10.1589/jpts.24.1359.

Islam, M. A., K. Sundaraj, R. B. Ahmad, N. U. Ahamed, and M. A. Ali. 2013. "Mechanomyography Sensor Development, Related Signal Processing, and Applications: A Systematic Review." IEEE Sensors Journal 13 (7): 2499–2516. https://doi.org/10.1109/JSEN.2013.2255982.

Jamal, Muhammad Zahak, and Kyung-Soo Kim. 2018. "A Finely Machined Toothed Silver Electrode Surface for Improved Acquisition of EMG Signals." In 2018 IEEE Sensors Applications Symposium (SAS), 1–5. Seoul: IEEE. https://doi.org/10.1109/SAS.2018.8336768.

Jiang, Xianta, Lukas-Karim Merhi, Zhen Gang Xiao, and Carlo Menon. 2017. "Exploration of Force Myography and Surface Electromyography in Hand Gesture Classification." Medical Engineering & Physics 41 (March): 63–73. https://doi.org/10.1016/j.medengphy.2017.01.015.

Junker, Holger, Oliver Amft, Paul Lukowicz, and Gerhard Tröster. 2008. "Gesture Spotting with Body-Worn Inertial Sensors to Detect User Activities." Pattern Recognition 41 (6): 2010–24. https://doi.org/10.1016/j.patcog.2007.11.016.

Kalantari, M., J. Dargahi, J. Kövecses, M. G. Mardasi, and S. Nouri. 2012. "A New Approach for Modeling Piezoresistive Force Sensors Based on Semiconductive Polymer Composites." IEEE/ASME Transactions on Mechatronics 17 (3): 572–81. https://doi.org/10.1109/TMECH.2011.2108664.

Kargov, Artem, Christian Pylatiuk, Jan Martin, Stefan Schulz, and Leonhard Döderlein. 2004. "A Comparison of the Grip Force Distribution in Natural Hands and in Prosthetic Hands." Disability and Rehabilitation 26 (12): 705–11. https://doi.org/10.1080/09638280410001704278.

Kim, Jongchan, Jungchul Lee, and Bumkyoo Choi. 2013. "Fabrication and Characterization of Strain Gauge Integrated Polymeric Diaphragm Pressure Sensors." International Journal of Precision Engineering and Manufacturing 14 (11): 2003–8. https://doi.org/10.1007/s12541-013-0272-y.

Lebosse, C., P. Renaud, B. Bayle, and M. de Mathelin. 2011. “Modeling and Evaluation of Low-Cost Force Sensors.” IEEE Transactions on Robotics 27 (4): 815–22. https://doi.org/10.1109/TRO.2011.2119850.

Li, Nan, Dapeng Yang, Li Jiang, Hong Liu, and Hegao Cai. 2012. “Combined Use of FSR Sensor Array and SVM Classifier for Finger Motion Recognition Based on Pressure Distribution Map.” Journal of Bionic Engineering 9 (1): 39–47. https://doi.org/10.1016/S1672-6529(11)60095-4.

Lobo-Prat, Joan, Peter N. Kooren, Arno HA Stienen, Just L. Herder, Bart FJM Koopman, and Peter H. Veltink. 2014. “Non-Invasive Control Interfaces Forintention Detection in Active Movement-Assistive Devices.” Journal of NeuroEngineering and Rehabilitation 11 (1): 168. https://doi.org/10.1186/1743-0003-11-168.

Lukowicz, Paul, Friedrich Hanser, Christoph Szubski, and Wolfgang Schobersberger. 2006. “Detecting and Interpreting Muscle Activity with Wearable Force Sensors.” In Pervasive Computing, edited by Kenneth P. Fishkin, Bernt Schiele, Paddy Nixon, and Aaron Quigley, 3968:101–16. Berlin, Heidelberg: Springer Berlin Heidelberg. https://doi.org/10.1007/11748625_7.

Matute, Arnaldo, Leonel Paredes-Madrid, Gelman Moreno, Fabián Cárdenas, and Carlos A. Palacio. 2018. “A Novel and Inexpensive Approach for Force Sensing Based on FSR Piezocapacitance Aimed at Hysteresis Error Reduction.” Research article. Journal of Sensors. 2018. https://doi.org/10.1155/2018/6561901.

Muhammed, H. H., and R. Jammalamadaka. 2016. “A New Approach for Rehabilitation and Upper-Limb Prosthesis Control Using Optomyography (OMG).” In 2016 1st International Conference on Biomedical Engineering (IBIOMED), 1–6. https://doi.org/10.1109/IBIOMED.2016.7869814.

Muhammed, Hamed Hamid, and Jammalamadaka Raghavendra. n.d. “Optomyography (OMG): A Novel Technique for the Detection of Muscle Surface Displacement Using Photoelectric Sensors,” 4.

Naik, Ganesh R., Suviseshamuthu Easter Selvan, Massimiliano Gobbo, Amit Acharyya, and Hung T. Nguyen. 2016. “Principal Component Analysis Applied to Surface Electromyography: A Comprehensive Review.” IEEE Access 4: 4025–37. https://doi.org/10.1109/ACCESS.2016.2593013.

Pancholi, S., and A. M. Joshi. 2018. “Portable EMG Data Acquisition Module for Upper Limb Prosthesis Application.” IEEE Sensors Journal 18 (8): 3436–43. https://doi.org/10.1109/JSEN.2018.2809458.

Paredes-Madrid, Leonel, Johanna Fonseca, Arnaldo Matute, Elkin I. Gutiérrez Velásquez, and Carlos A. Palacio. 2018. “Self-Compensated Driving Circuit for Reducing Drift and Hysteresis in Force Sensing Resistors.” Electronics 7 (8): 146. https://doi.org/10.3390/electronics7080146.

Radmand, Ashkan, Erik Scheme, and Kevin Englehart. 2016. “High-Density Force Myography: A Possible Alternative for Upper-Limb Prosthetic Control.” Journal of Rehabilitation Research and Development 53 (4): 443–56. https://doi.org/10.1682/JRRD.2015.03.0041.

Schoening, Herbert A. 1986. “Muscles Alive—Their Function Revealed by Electromyography (5th Edition): By John V. Basmajian and Carlo J. Deluca. Hardcover. Price $45.00. 561 Pages. Williams and Wilkins, PO Box 969, Waverly Press Lane, Easton, MD 21601.”

Archives of Physical Medicine and Rehabilitation 67 (4): 240. https://doi.org/10.5555/uri:pii:0003999386903758.
Searle, A., and L. Kirkup. 2000. “A Direct Comparison of Wet, Dry and Insulating Bioelectric Recording Electrodes.” Physiological Measurement 21 (2): 271. https://doi.org/10.1088/0967-3334/21/2/307.
Sharma, Tanu, and Karan Veer. 2016. “Design and Optimization of Neural Classifier to Identify around Shoulder Motions.” Optik 127 (7): 3564–68. https://doi.org/10.1016/j.ijleo.2016.01.007.
Spires, M. Catherine, Brian Kelly, and Alicia J. Davis, eds. 2014. Prosthetic Restoration and Rehabilitation of the Upper and Lower Extremity. New York: Demos Medical.
Supuk, Tamara Grujic, Ana Kuzmanic Skelin, and Maja Cic. 2014. “Design, Development and Testing of a Low-Cost SEMG System and Its Use in Recording Muscle Activity in Human Gait.” Sensors (Basel, Switzerland) 14 (5): 8235–58. https://doi.org/10.3390/s140508235.
Tavakoli, Mahmoud, Carlo Benussi, and Joao Luis Lourenco. 2017. “Single Channel Surface EMG Control of Advanced Prosthetic Hands.” Expert Syst. Appl. 79 (C): 322–332. https://doi.org/10.1016/j.eswa.2017.03.012.
Veer, Karan. 2014. “INTERPRETATION OF SURFACE ELECTROMYOGRAMS TO CHARACTERIZE ARM MOVEMENT.” Instrumentation Science & Technology 42 (5): 513–21. https://doi.org/10.1080/10739149.2014.913178.
Veer, K., 2015. “Experimental Study and Characterization of SEMG Signals for Upper Limbs.” Fluctuation and Noise Letters 14 (03): 1550028. https://doi.org/10.1142/S0219477515500285.
Veer, Karan, Ravinder Agarwal, and Amod Kumar. 2016. “Processing and Interpretation of Surface Electromyogram Signal to Design Prosthetic Device.” Robotica 34 (7): 1486–94. https://doi.org/10.1017/S0263574714002409.
Veer, Karan, and Tanu Sharma. 2018. “Electromyographic Classification of Effort in Muscle Strength Assessment.” Biomedical Engineering / Biomedizinische Technik 63 (2): 131–37. https://doi.org/10.1515/bmt-2016-0038.
Woodward, Richard B., Maria J. Stokes, Sandra J. Shefelbine, and Ravi Vaidyanathan. 2019. “Segmenting Mechanomyography Measures of Muscle Activity Phases Using Inertial Data.” Scientific Reports 9 (1): 5569. https://doi.org/10.1038/s41598-019-41860-4.
Xiao, Zhen G, and Carlo Menon. 2014. “Towards the Development of a Wearable Feedback System for Monitoring the Activities of the Upper-Extremities.” Journal of NeuroEngineering and Rehabilitation 11 (1): 2. https://doi.org/10.1186/1743-0003-11-2.
Xiao, Zhen Gang, and Carlo Menon. 2019. “An Investigation on the Sampling Frequency of the Upper-Limb Force Myographic Signals.” Sensors 19 (11): 2432. https://doi.org/10.3390/s19112432.
Yaniger, S. I. 1991. “Force Sensing Resistors: A Review Of The Technology.” In Electro International, 1991, 666–68. https://doi.org/10.1109/ELECTR.1991.718294.